

Synthesis, Characterization and Decomposition of 4-Diazo-2,6-dinitrophenol

Jian-long Wang,^{*,[a]} Cai Cao,^[a] Jun-yan Cao,^[b] Yu-min Yan,^[c] Li-zhen Chen,^[a] and Duan-lin Cao^[a]

Abstract: A high energetic compound 4-diazo-2,6-dinitrophenol was synthesized by employing one-pot facile method from 4-chloro-3,5-dinitroaniline. Its structure was characterized by Fourier transform infrared spectroscopy (FT-IR), elemental analysis (EA), and nuclear magnetic resonance spectroscopy (¹H NMR, ¹³C NMR and ¹⁵N NMR). The crystal structure was determined using an X-ray single crystal diffractometer. The detonation properties of 4-diazo-2,6-

dinitrophenol and 6-diazo-3,5-dichloro-2,4-dinitrophenol were compared by using Kamlet formula. Besides, the thermal behavior of 4-diazo-2,6-dinitrophenol was analyzed by differential scanning calorimetry (DSC) and accelerating rate calorimeter (ARC), then according to the thermal analysis data, the thermal decomposition kinetics parameters were calculated using the thermal analysis data based on Kissinger method and Flynn-Wall-Ozawa method.

Keywords: 4-Diazo-2,6-dinitrophenol • Crystal structure • Detonation velocity • Thermal Decomposition

1 Introduction

Energetic materials (EMs) are typical small molecular organic compounds that can store and rapidly release a large amount of chemical energy [1]. Over the past few decades, a variety of high-energy substances have been reported, among which the high-nitrogen EMs have attracted more attention because they are more environmentally friendly and have higher energy than traditional nitramine explosives [2–3]. With the development of modern society, modern explosives and propellants must be high-density, environmentally friendly and rich in nitrogen and oxygen. Therefore, the molecular design of EMs requires a variety of energetic functional groups, such as azido, diazo, nitro groups and perchlorate, et al. [4–5]. Due to the fact that nitro and diazo compounds can release a lot of gas and energy during high energy decomposition, they are widely used in civilian and military fields [6]. A new class of N₂⁺ compounds in the field of EMs has attracted great interest. These compounds exhibit high positive heat of formation which is attributed to the presence of a large number of N–N and C–N bounds. In addition, nitro and diazo groups can improve the density and oxygen balance of these compounds, thus improving their detonation properties [7].

In recent years, there are many reports about the thermal performance tests and analysis of energetic compounds. The synthesis, thermal analysis, and calculation of impact sensitivity and detonation parameters of promising insensitive energetic compounds of 4-chloro-3,5-dinitropyrazole were reported by He et al. [7] It fully indicated that the substance has high density, good thermal stability, and excellent detonation performance. The synthesized multi-nitro compound of 1,1-diamino-4,4,5,5-tetranitro-2,2-biimidazole by a one-pot method was reported by Ma et al. [8],


and its thermal decomposition mechanism was studied by DSC and TG-FTIR techniques. It is considered that the substance may be a substitute for high energy insensitive explosive. The synthesis and thermal behavior of 3-nitro-4-diazo-5-oxygenpyrazole, a diazo heterocyclic compound with poor thermal stability, have been reported by Chen et al. [9]. The thermal behavior and safety of the new high temperature explosive of 5,5',6,6'-tetranitro-2,2'-bibenzimidazole (TNBBI) were investigated by DSC, and the kinetic parameters of TNBBI at the initial stage of decomposition were measured by Tomasz Gołofit et al. [10].

The thermal decomposition of EMs is a complex process containing physical and chemical transformation [11–12]. DSC is a common method to study the non-isothermal thermal decomposition of liquids and solids [13], and ARC is an effective instrument to investigate the adiabatic thermal decomposition process of materials [14]. The apparent acti-

[a] J.-l. Wang, C. Cao, L.-z. Chen, D.-l. Cao
School of Chemical Engineering and Technology, North University of China, 030051, Taiyuan, China
*e-mail: wangjianlong@nuc.edu.cn
18434365967@163.com
chen17555@163.com
cdl@nuc.edu.cn

[b] J.-y. Cao
Sichuan Aerospace Changzheng Equipment Manufacturing Co., Ltd., 610100, Chengdu, China
*e-mail: 578678997@qq.com

[c] Y.-m. Yan
China North Xing'an Chemical Industry Co., Ltd., 030051, Taiyuan, China
*e-mail: 294840225@qq.com

 Supporting information for this article is available on the WWW under <https://doi.org/10.1002/prep.202100005>

vation energy (E) and the pre-exponential factor (A) are the main parameters to reflect the thermal decomposition performance of EMs.

The synthesis and characterization of dinitrodiazoquinone which is closely related to 4-diazo-2,6-dinitrophenol were reported by Bergman [15], and the synthesis mechanism was also described through nitramine rearrangement. A paper discussing the increased-valence bond structure of 2-diazo-4,6-dinitrophenol (DDNP), as opposed to the zwitterionic approach, was published in 2003 by Klapötke et al. [16]. In addition, the 4-fluorobenzoic acid was used as a raw material to synthesize 4-fluoro-3,5-dinitroaniline via Schmidt reaction [17]. A two-step reaction of amination and nitration to synthesize the target compound 4-diazo-2,6-dinitrophenol in 2015 by the same group. DDNP and 4-diazo-2,6-dinitrophenol both have potential as a primary explosive or detonator. In this paper, 4-chlorobenzoic acid was used as raw material to synthesize 4-chloro-3,5-dinitroaniline through Schmidt reaction, and then the target compound was obtained by nitration reaction. Compared with the synthetic route of Klapötke, this method has many advantages, such as simpler, shorter reaction times, fewer solvents, lower cost and easier access to raw materials. Besides, 4-diazo-2,6-dinitrophenol is a very interesting energetic zwitterionic molecule. Most compounds containing a nitro group in *ortho* position to a nitramine functionality eliminate nitric acid during the nitration reaction or boiling process in organic solvents. The rearrangement of nitroaromatic nitramines results in the formation of *ortho*-diazophenols [18]; the reaction process is shown in Scheme 1. Similarly, after the two-step synthesis of 4-fluoro-3,5-dinitroaniline, two steps are needed to obtain *para*-diazophenol as confirmed by Klapötke, and the synthesis route is shown in Scheme 2. However, the compound of 4-diazo-2,6-dinitrophenol was synthesized in one step using 4-chloro-3,5-dinitroaniline as the raw material in this paper, without the need to synthesize 4-amino-3,5-dinitroaniline. Therefore, a new conclusion is obtained: the nitro group and the amino group that are *meta* positions and the en-

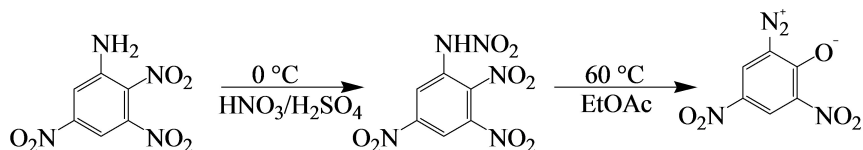
ergetic *para*-diazophenol can also be synthesized by a rearrangement reaction.

2 Experimental Section

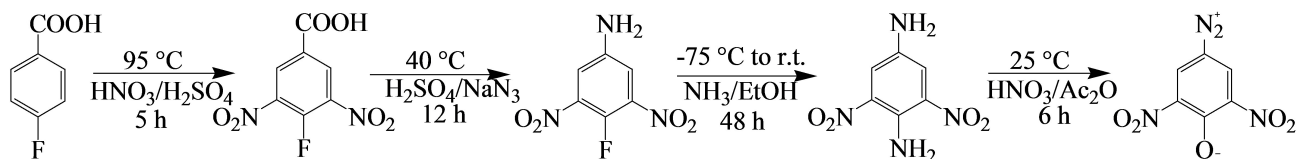
2.1 Materials and Instruments

All Reagents: Fuming nitric acid (Tech, 98.0%) and sulfuric acid (Tech, 20%) were purchased from China North Xing'an Chemical Industry Co., Ltd. Trichloromethane (AR, 99.5%), acetic acid, petroleum ether (AR, 99.5%) and ethyl acetate (AR, 99.5%) were purchased from Xilong Scientific Co., Ltd. China, and used without further purification. 4-Chlorobenzoic acid was purchased from Sinopharm Chemical Reagent Co., Ltd., China. Sodium azide and sodium dichloroisocyanurate (SDCI) were purchased from Tianjin Fengchuan Chemical Reagent Technology Co., Ltd., China. The distilled water was made in the laboratory. The 4-chloro-3,5-dinitroaniline were prepared at North University of China according to the method of Yang et al. [19–20].

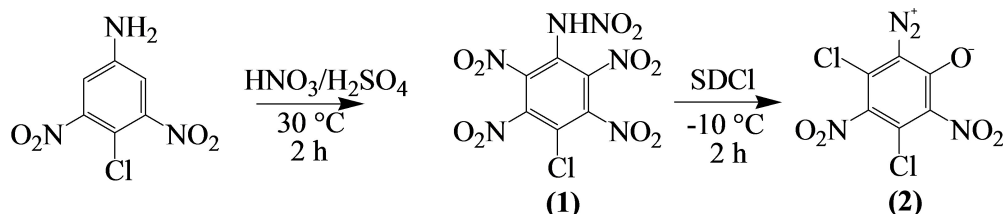
Test Instrument: The melting point was measured on a M-565 melting point apparatus provided by BUCHI Company in Switzerland. The FT-IR spectra were measured on a VERTEX 80 produced by Bruker in Germany. The elemental analyses were taken on an Elementar Vario EL cube produced by Elementar Company in Germany. ^1H NMR, ^{13}C NMR and ^{15}N NMR spectra were detected with an AVANCE IIIITM 600 MHz manufactured by Bruker Company in Switzerland using $\text{DMSO-}d_6$ (the reference compound is tetramethylsilane) as solvent. The impact sensitivity (IS) and friction sensitivity (FS) were determined by using a CGY-1 impact sensitivity meter and an MGY-1 friction sensitivity meter in accordance with the standard GJB 5891.22-2006 and GJB 5891.24-2006 [21–22]. The electrostatic discharge sensitivity tests were performed using a JGY-50II electrostatic discharge (ESD) instrument according to GJB 5891.27-2006 [21]. X-ray single-crystal diffraction data were collected on a "Bruker APEX-II CCD" diffractometer. Thermal



Scheme 1. The synthetic route of the *ortho*-diazophenols.



Scheme 2. The synthetic route of the *para*-diazophenols by Klapötke.



Scheme 3. The synthetic route of the compound (2).

performance analysis instruments were METTLER DSC 3 and ES-ARC.

2.2 Synthesis

4-Chloro-1-amino-2,3,5,6-tetranitrobenzene (1): 4-chloro-3,5-dinitroaniline (5 g, 23 mmol) was added to the mixed solution of sulfuric acid (80 mL, 98%) and nitric acid (8 mL, 98%) at below 25 °C. Then stirred at 30 °C for 2 h. After the reaction, the mixture was poured into crushed ice to produce a large amount of yellow solid precipitate, which was filtered and washed with petroleum ether to obtain 5.7 g yellow solid, with a yield of 69.1%. The synthetic route of the compound is shown in Scheme 3. Anal. FT-IR (KBr pellet, ν/cm^{-1}): 3424.41 (Ar-N), 1625.21 (N-H), 1564.98, 1343.04 (Ar-NO₂), 770.71 (C-Cl) (see Figure 1S, Supporting documents). Calcd. (%) for C₆H₃O₁₀N₆Cl (molecular weight: 352.5): C 20.43, H 0.28, N 23.83, O 45.39, Cl 10.07. found (%): C 20.50, H 0.30, N 23.81.

6-Diazo-3,5-dichloro-2,4-dinitrophenol (2) [23]: The compound (1) (5 g, 14 mmol) was added to 100 mL acetonitrile.

To this solution, a mixture of SDCI (23 mmol) and AcOH (5 mL) in water (100 mL) was added dropwise at 0–5 °C. After addition, the reaction was stirred for 2 h at –10 °C. The solid was gradually precipitated and filtered to obtain 1.1 g solid with a yield of 28.2%. The synthetic route of the compound is shown in Scheme 3. Anal. FT-IR (KBr pellet, ν/cm^{-1}): 2177.18 (–N₂), 1634.61 (C=O), 1538.86, 1353.82 (–NO₂), 709.84 (C–Cl) (see Figure 2S, Supporting documents) Calcd. (%) for C₆N₄O₅Cl₂ (molecular weight: 279.0): C 25.81, H 0, N 20.07, O 28.67, Cl 25.45. Found (%): C 25.98, N 20.08.

4-Diazo-2,6-dinitrophenol (3): 4-chloro-3,5-dinitroaniline (5 g, 23 mmol) was added to 100 mL of nitric acid (98%) at below 25 °C. Then stirred for 2 h at room temperature and gradually raised the temperature to 63 °C and heat 2 h. After the reaction, poured the mixture into the ice water, then some yellow crystals were precipitated slowly, filtered and dried to give 4-diazo-2,6-dinitrophenol (3), the yield was 67%, and the decomposition temperature was 190–191 °C. The synthetic route of the compound is shown in Scheme 4. Anal. FT-IR (KBr pellet, ν/cm^{-1}): 1535.16, 1359.47 (–NO₂), 1641.46 (C=O), 1619.34 (C=N), 2187.21 (N≡N) (see Figure 3S, Supporting documents). ¹H NMR (600 MHz, DMSO-*d*₆) δ : 8.97 ppm. ¹³C NMR (151 MHz, DMSO-*d*₆) δ : 161.34, 143.12, 132.72, 81.42 ppm. ¹⁵N NMR (61 MHz, DMSO-*d*₆) δ : –13.46, –45.63, –138.23 ppm. (see Figure 4S, Supporting

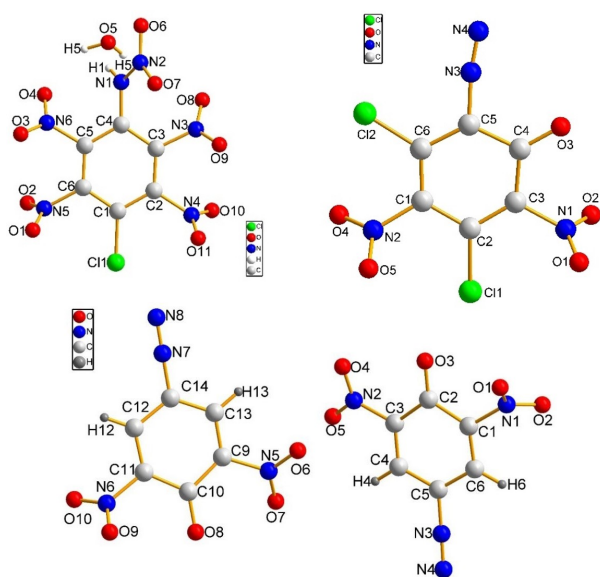


Figure 1. Molecular structure of the compound (1), (2) and (3).

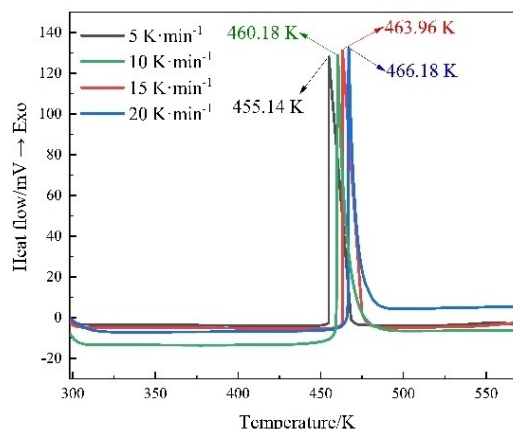
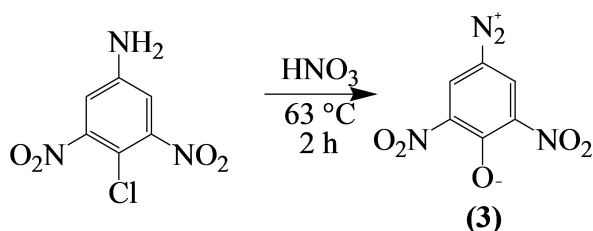


Figure 2. DSC curves of the compound (3) at different heating rates.



Scheme 4. The synthetic route of the compound (3).

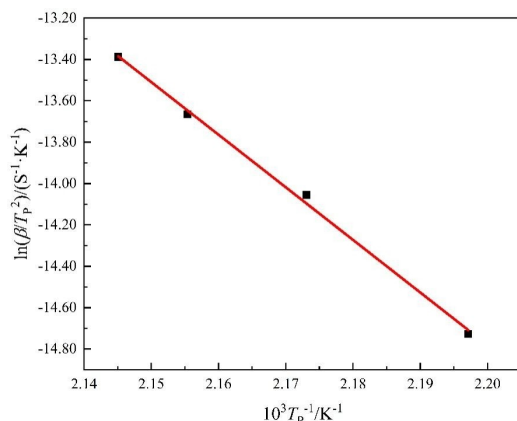


Figure 3. $\ln(\beta/T_p^2)$ versus T_p^{-1} by Kissinger method of the decomposition.

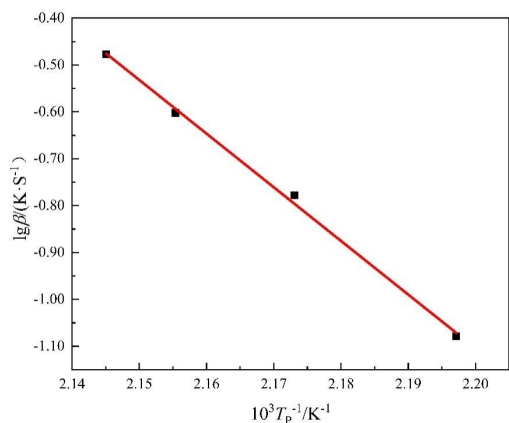


Figure 4. $\lg \beta$ versus T_p^{-1} by FWO method of the decomposition.

documents). Calcd. (%) for $\text{C}_6\text{H}_2\text{O}_5\text{N}_4$ (molecular weight: 210.0): C 34.29, H 0.95, N 26.67, O 38.09. Found (%): C 34.17, H 0.95, N 26.29. Sensitivities (grain size < 100 μm): IS 1 J, FS 40 N, ESD 228mJ.

2.3 Crystal Structure Determination

Single crystals suitable for X-ray measurement were obtained by slow evaporation of their saturated solutions in

water at room temperature. The single crystals of compounds (1), (2) [23] and (3) with appropriate size were selected to determine its structure on a Bruker APEX-II CCD diffractometer. A graphite monochromator ray of Mo $K\alpha$ radiation ($\lambda = 0.71073$ nm) at a temperature of 170 K were applied to scan. The total numbers of diffraction spots and the numbers of independent diffraction spots collected by multi-scan scanning method are shown in the Table 1S (see Supporting documents). Using Olex2 [24], the structure was solved with the ShelXT [25] structure solution program using Intrinsic Phasing and refined with the ShelXL [26] refinement package using Least Squares minimisation.

2.4 Calculation of Detonation Velocity and Detonation Pressure

In this paper, density function theory (DFT) method was used to calculate the heat of formation of the compound (2) and (3) at the B3LYP/6-31 + G** level in combination with the design of equal bond reaction. The detonation velocities and detonation pressures were calculated by the Kamlet formula [27–28], the relevant data are shown in Table 1.

2.5 Thermal Experimental Instruments and Conditions

The non-isothermal thermal analysis was carried out on DSC at heating rates of 5, 10, 15, 20 $\text{K} \cdot \text{min}^{-1}$ from 298.15 K to 573.15 K [29] in a nitrogen atmosphere with a flow rate of 50 $\text{mL} \cdot \text{min}^{-1}$. The mass of the compound (3) was 0.7–0.8 mg.

The ARC is one of the important instruments to evaluate the thermal stability of substances. Compared with DSC, the added dosage of ARC test can reach the g-level and the detection sensitivity is high, resulting in more accurate results. ARC test was performed on the compound (3) using Hastelloy pellet (type: HC-LCQ) with a mass of 14.7363 g and specific heat of 0.42 $\text{J} \cdot \text{g}^{-1} \cdot \text{K}^{-1}$. The test temperature ranges from 40 to 400 $^{\circ}\text{C}$. The heating step was 5 $^{\circ}\text{C}$, the sensitivity was 0.02 $^{\circ}\text{C} \cdot \text{min}^{-1}$. The mass of the compound (3) in the pellet was 0.076 g, and its specific heat capacity was estimated as 1.21 $\text{J} \cdot \text{g}^{-1} \cdot \text{K}^{-1}$ by Kopp law [30].

3 Results and Discussion

3.1 Crystal Structure Description

The crystal data and structure refinement parameters of compound (1), (2) and (3) are listed in Table 1S (see Supporting documents), the bond lengths, bond angles and torsion angles of compound (3) are shown in the Tables 2S and 3S (see Supporting documents). The crystal structures of compound (1), (2) and (3) are shown as Figure 1, and

Table 1. The detonation parameters of compound (2), (3), TNT and RDX.

Compound	Characteristic value (ϕ)	Molar mass ($M/\text{g} \cdot \text{mol}^{-1}$)	Density ($\rho/\text{g} \cdot \text{cm}^{-3}$)	Detonation heat ($Q/\text{kJ} \cdot \text{kg}^{-1}$)	Detonation velocity ($D/\text{m} \cdot \text{s}^{-1}$)	Detonation pressure (P/GPa)
compound (2)	7.999	279.00	1.907	5668	6949	23.42
compound (3)	10.826	210.12	1.813	6387	7800	27.85
TNT	9.896	227.13	1.654	4226	6947	20.12
RDX	13.877	222.12	1.800	6016	8750	32.63

The relevant substance data in the above table comes from <https://wenku.baidu.com/view/a73c3a90846a561252-d380eb6294dd88d0d23dc4.html>.

Table 2. Data of the compound (3) obtained by DSC curves at different heating rates.

Heating rate ($\beta/(\text{K} \cdot \text{min}^{-1})$)	Peak temperature ($T_p/(\text{K})$)	$10^3 T_p^{-1}/(\text{K}^{-1})$	Kissinger method $\ln((\beta/T_p^2)/(\text{K}^{-1} \cdot \text{s}^{-1}))$	FWO method $\lg(\beta/(\text{K} \cdot \text{s}^{-1}))$
5	455.14	2.1971	−14.7261	−1.0792
10	460.18	2.1731	−14.0550	−0.7782
15	463.96	2.1554	−13.6659	−0.6021
20	466.18	2.1451	−13.3878	−0.4771

three-dimensional crystal packing of compound (3) is shown as Figure 5S. (see Supporting documents). Figure 5S shows that there are sixteen ordered molecular structures of the compound (3) in a unit cell.

The single crystal analysis shows that the compound (3) belongs to orthorhombic with the space group of $P2_12_12_1$ and the crystal density is $1.813 \text{ g} \cdot \text{cm}^{-3}$. As shown in Figure 1, the N1, N2, N3 are connected to C1, C3 and C5, respectively. The bond lengths of N1-C1, N2-C3 and N3-C5 are 1.471, 1.458 and 1.372 Å, respectively (see Table 2S. Supporting documents), which indicates that the diazo group is more stable than nitro groups. The dihedral angles between the six atoms of the ring and two nitro groups are 48.494° and 81.859° , respectively, which suggests that the coplanarity of six atoms of the ring and the two nitro

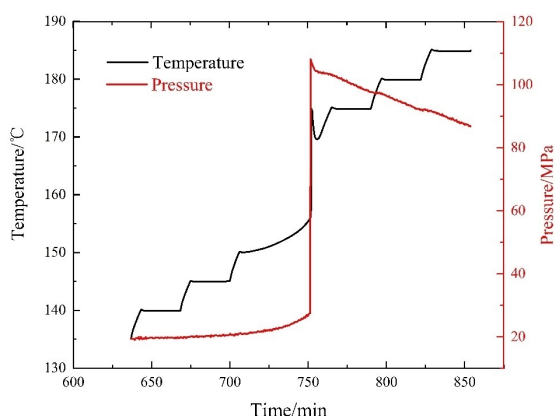
groups is relatively poor. In addition, the bond angles indicate that the structure of the compound (3) is opposite symmetry (see Table 2S. Supporting documents). The torsion angles of C1-C2-C3-C4, C2-C3-C4-C5, C3-C4-C5-C6, C4-C5-C6-C1, C5-C6-C1-C2, C6-C1-C2-C3 of the compound (3) are $-4.161(455)^\circ$, $1.520(446)^\circ$, $1.443(440)^\circ$, $-2.052(453)^\circ$, $-0.200(425)^\circ$ and $3.469(421)^\circ$, respectively (see Table 3S. Supporting documents). It demonstrates that the structure of the compound (3) has certain stability because of its symmetry.

3.2 Calculation Results of Detonation Parameters

At the B3LYP/6-31 + G** level of DFT, the compound 2-diazophenol and 4-diazophenol are selected as the parent respectively, and the isodesmic reactions are designed as shown in Scheme 1S and 2S (see Supporting documents). And the total energy (E_0), zero-point energy (ZPE), and thermal correction to enthalpy (H_T) of the compound (2) and (3) are accurately calculated by using Gaussian 09, respectively (see Table 4S. Supporting documents). The empirical formulas for calculating explosive detonation velocity and detonation pressure proposed by Kamlet are as follows:

$$D = 0.7062 \varphi^{\frac{1}{2}} (1 + 1.30\rho) \quad (1)$$

$$P = 7.617 \times 10^8 \varphi \rho^2 \quad (2)$$

**Figure 5.** Temperature and pressure versus time.**Table 3.** Kinetics parameters of thermal decomposition of the compound (3) by DSC.

Parameters	Decomposition
Apparent activation energy by Kissinger method ($E_k/(\text{kJ} \cdot \text{mol}^{-1})$)	211.43
Pre-exponential factor by Kissinger method ($A/(\text{s}^{-1})$)	1.92×10^{22}
Square of the correlation coefficient by Kissinger method (r_k^2)	0.9976
Apparent activation energy by FWO method ($E_o/(\text{kJ} \cdot \text{mol}^{-1})$)	208.34
Square of the correlation coefficient by FWO method (r_o^2)	0.9978

Table 4. Self-heating decomposition parameters of the compound (3) by ARC.

Parameters	Values	Corr.
Onset temperature/°C	150.91	–
Onset temperature rate/°C min ^{−1}	0.081	5.53
Max self-heating rate/°C min ^{−1}	1406.23	96045.51
Temperature at max rate/°C	164.70	1092.77
Final temperature/°C	175.19	1659.01
Adiabatic temperature rise/°C	24.29	1809.92
Time to maximum rate/min	28.64	0.42
Onset pressure/MPa	0.219	–
Pressure at max rate/MPa	1.082	–
Decomposition heat/J·g ^{−1}	29.39	2190.00

where ϕ is the characteristic value of the explosive, $\phi = NM^2Q^2/\rho$; ρ is the explosive density, g·cm^{−3}; D is the detonation velocity of an explosive with a density of ρ , km·s^{−1}; N is the molar mass of gas detonation products of per gram explosive, mol·g^{−1}; M is the average molar mass of gas detonation products, g·mol^{−1}; Q is the explosive chemical energy per gram of the explosive, that is, the maximum detonation heat per unit mass, J·g^{−1}; P refers to the detonation pressure of the explosive, Pa.

The detonation parameters of compound (2), (3), TNT and RDX are listed in Table 1 for comparison. It can be seen that the detonation velocity and detonation pressure of compound (3) are all higher than the compound (2) and TNT, the detonation heat is higher than RDX, which indicates that the compound (3) has better detonation performance. The results show that the compound (3) is an excellent energetic material. Therefore, the thermal properties of the compound (3) were further analyzed.

3.3 Thermal Behavior of the Title Compound

3.3.1 The Thermal Analysis of DSC Results

The exothermic curves of compound (3) at different heating rates are shown in Figure 2. It can be clearly seen from the DSC curves that the compound has only one exothermic peak, of which the heat release rapidly and greatly. The exothermic decomposition peaks at the heating rates of 5, 10, 15 and 20 K·min^{−1} are 455.14 K, 460.18 K, 463.96 K and 466.18 K, respectively. The ΔH_d is 4069.96 J·g^{−1}.

The apparent activation energy (E) and the pre-exponential factor (A) of the compound (3) were calculated by Kissinger method [31] and Flynn-Wall-Ozawa method [32]. The Kissinger and FWO equations are as follows:

$$\ln\left(\frac{\beta}{T_p^2}\right) = \ln\left(\frac{AR}{E}\right) - \frac{E}{RT_p} \quad (3)$$

$$\lg\beta = \lg\left[\frac{AE}{RG(\alpha)}\right] - 2.315 - \frac{0.4567E}{RT_p} \quad (4)$$

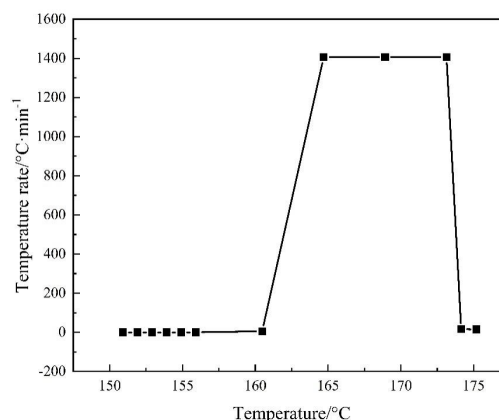
where β is the linear heating rate (K·min^{−1}), T_p is the peak temperature of the DSC curves (K), A is the pre-exponential factor (s^{−1}), R is the gas constant (J·mol^{−1}·K^{−1}), E is the apparent activation energy (kJ·mol^{−1}), $G(\alpha)$ is the integral form of reaction mechanism function [33].

According to Eqs. (3) and (4), $\ln(\beta/T_p^2)$ and $\lg\beta$ varies linearly with $1/T_p$, respectively. The data fitting results are shown in Figure 3 and Figure 4. The kinetic parameters E and A calculated according to Kissinger method are 211.43 kJ·mol^{−1} and 1.92×10^{22} s^{−1}, respectively, and the r_k^2 is 0.9976. The E_o calculated by FWO method is 208.34 kJ·mol^{−1} and r_o^2 is 0.9978. The data are shown in Tables 2 and 3. It can be seen that the E calculated by the two methods are relatively close, and the correlation coefficient is close to 1, indicating the reliability of the data results.

3.3.2 The Thermal Analysis of ARC Results

Thermal decomposition results of compound (3) tested by ARC in an adiabatic environment are shown in Figure 5 and Figure 6. With the progress of the experiment, the thermal decomposition rate (temperature rise rate) of the compound increases sharply. A large amount of gas is generated during the thermal decomposition process, leading to the sharp increase of system pressure. The pressure change is consistent with the temperature, which indicates that the catalytic products are produced during the thermal decomposition process, which greatly accelerates the decomposition rate.

In the ARC test, the heat released by the sample not only heats the sample itself, but also heats the test ball, so thermal inertias are required to correct the data. The following thermodynamic equilibrium exists between the sample and the reactor:


Figure 6. Decomposition temperature rate verse temperature.

$$MC_V\Delta T_{AB} = (M_b C_{V,b} + MC_V)\Delta T_{AB,s} \quad (5)$$

Here, M is the sample mass, g; C_V is specific heat capacity of the sample, $J \cdot g^{-1} \cdot K^{-1}$; ΔT_{AB} is the adiabatic temperature rise, $^{\circ}C$; M_b is the mass of the ball, g; $C_{V,b}$ is specific heat capacity of the pellet, $J \cdot g^{-1} \cdot K^{-1}$. It can be obtained from Eq. (5):

$$\Delta T_{AB} = \left(1 + \frac{M_b C_{V,b}}{MC_V}\right) \Delta T_{AB,s} \quad (6)$$

Here, $\Phi = 1 + \frac{M_b C_{V,b}}{MC_V}$, is the thermal inertia factor of the sample reactor. The corrected equations for the decomposition parameters are shown as follows:

$$\Delta T_{AB} = \Phi \Delta T_{AB,s} \quad (7)$$

$$T_f = T_0 + \Phi \Delta T_{AB,s} \quad (8)$$

$$\theta = \frac{\theta_s}{\Phi} \quad (9)$$

$$m_T = \Phi m_{T,s} \quad (10)$$

$$\Delta H = \Phi \Delta H_s \quad (11)$$

Here, the subscript 0 is the initial state, the subscript f is the final state, θ is the time to reach the maximum speed, m_T is the adiabatic temperature rise rate, the subscript s is measured value.

The adiabatic decomposition parameters corrected according to the Φ before and after calibration values are shown in Table 4. The results show that the compound (3) has only one exothermic phase with the initial decomposition temperature of $150.91^{\circ}C$, adiabatic temperature rise of $24.29^{\circ}C$, the maximum self-heating rate of $1406.23^{\circ}C \cdot \min^{-1}$ and decomposition heat of $29.39 J \cdot g^{-1}$, respectively. The corrected data show that adiabatic temperature rise is $1809.92^{\circ}C$, the maximum self-heating rate of the compound (3) during adiabatic decomposition is $96045.51^{\circ}C \cdot \min^{-1}$ and the decomposition heat is $2190.00 J \cdot g^{-1}$.

The data processing of the adiabatic accelerometer is based on the method developed by Gigante et al. [34] The

reaction rate and temperature are in accordance with the Arrhenius formula:

$$k = Ae^{(-E/RT)} \quad (12)$$

Here, k is the reaction rate constant, A is the pre-exponential factor, E is the apparent activation energy, R is the gas constant, and T is the temperature. Then define a quasi-rate constant k^* :

$$k^* = kc_0^{n-1} = \frac{m_T}{\Delta T_{AB}} \left(\frac{T_f - T}{\Delta T_{AB}}\right)^{-n} \quad (13)$$

Here, c represents the reaction concentration; n is the series of reactions. Then the Eq. (14) can be obtained by combining Eq. (12) and Eq. (13):

$$\ln k^* = \ln \frac{m_T}{\Delta T_{AB} \left(\frac{T_f - T}{\Delta T_{AB}}\right)^n} = \ln A - \frac{E}{RT} \quad (14)$$

According to Eq. (14), $1/T$ is fitted linearly with $\ln k^*$, and the fitting curves obtained are shown in Figure 7. The E and A are calculated from the slope $-E/R$ and the intercept $\ln A$. The correlation coefficient r^2 , E and A under different reaction orders are shown in Table 5. The results show that when n is 2, the linear fitting is good with the correlation

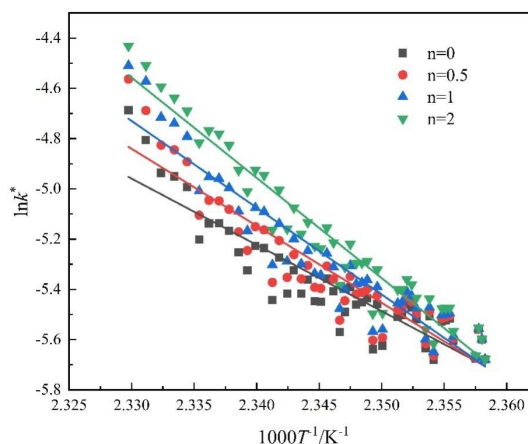


Figure 7. $\ln k^*$ versus T^{-1} of the decomposition of the title compound.

Table 5. Thermal decomposition kinetic parameters of the compound (3) by ARC.

Order of reaction (n)	Intercept (ln A)	Slope (-E/R)	Square of the correlation coefficient (r^2)	Pre-exponential factor ($A/(s^{-1})$)	Apparent activation energy ($E/(kJ \cdot mol^{-1})$)
0	56.4713	-26.3651	0.8291	3.35×10^{24}	219.21
0.5	66.5551	-30.6419	0.8654	8.03×10^{28}	254.77
1	75.7118	-34.5242	0.8968	7.61×10^{32}	287.05
2	88.3898	-39.8914	0.9468	2.44×10^{38}	331.68

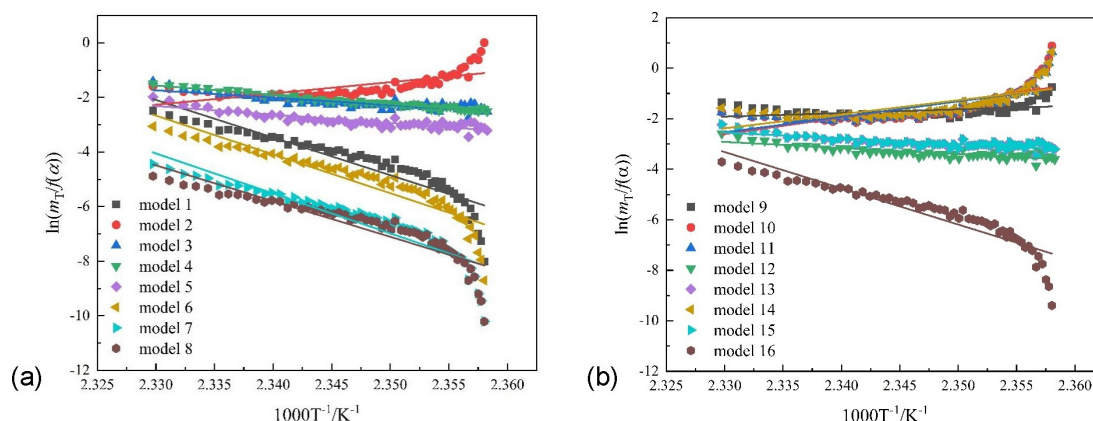


Figure 8. The model fitting curves for the decomposition of the compound (3): (a) 1–8; (b) 9–16.

coefficient r^2 of 0.9468. The E and A are $331.68 \text{ kJ} \cdot \text{mol}^{-1}$ and $2.44 \times 10^{38} \text{ s}^{-1}$, respectively.

The apparent activation energy E and pre-exponential factor A of adiabatic decomposition can also be calculated by the mechanism function method [35], and the formula is as follows:

$$\ln \left[\frac{m_T}{f(\alpha)} \right] = \ln(A \Delta T_{AB}) - \frac{E}{RT} \quad (15)$$

Here, $\alpha = \frac{c_0 - c}{c_0} = \frac{T - T_0}{\Delta T_{AB}}$, is the reaction degree; $f(\alpha)$ represents 16 different mechanism function models (see Table S5. Supporting documents). Substitute the experimental data into 16 models, then the model fitting curves of compound (3) were obtained (Figure 8). In these curves, the slope is $-E/R$ and the intercept is $\ln(A \Delta T_{AB})$. Therefore, 16 sets of kinetic parameter regression data for the decomposition can be obtained (see Table S6. Supporting documents). The highest correlation coefficient and the corresponding kinetic model are obtained when model 4 is chosen. As a result, the thermal decomposition mechanism of compound (3) is $f(\alpha) = (1 - \alpha)^2$, the E and A calculated are $279.58 \text{ kJ} \cdot \text{mol}^{-1}$ and $9.00 \times 10^{31} \text{ s}^{-1}$, respectively.

4 Conclusions

The following conclusions can be drawn from this experimental study: The target compound 4-diazo-2,6-dinitrophenol (3) can be obtained through a one-step reaction of rearrangement from 4-chloro-3,5-dinitroaniline, the step of synthesis is fewer and the experimental conditions are easier to achieve than the Klapötke's method. The crystal structure of the compound (3) is obtained by an X-ray single crystal diffractometer, and the detonation parameters and thermal properties of the compound (3) are studied simultaneously. The results show that the compound (3) belongs to orthorhombic with the space group of $P2_12_12_1$. The detonation properties and thermal performance show that

the compound (3) has higher energy than the compound (2) and excellent thermal stability. Therefore compound (3) has the potential as the energetic primary explosive or detonator due to its rapid heat release, high energy, high density and good stability.

Acknowledgements

We are grateful for the Center of Testing and Analysis, Shanghai Institute of Materia Medica for support.

Data Availability Statement

The data used to support the findings of this study are included within the article.

References

- [1] H. X. Gao, J. M. Shreeve, Azole-based energetic salts, *Chem. Rev.* **2011**, *111*, 7377–7436. <https://doi.org/10.1021/cr200039c>.
- [2] S. M. Jin, Y. C. Liu, D. C. Liu, J. H. Guo, Study on quantum chemistry of structure and properties of a novel high energetic density compound BNFDAONAB, *Initiators & Pyrotechnics*. **2015**, *2*, 41–43.
- [3] Q. L. Yan, L. L. Liu, W. He, C. J. Luo, A. Shlomovich, P. J. Liu, J. Kong, M. Gozin, Decomposition kinetics and thermolysis products analyses of energetic diaminotriazole-substituted tetrazine structures, *Thermochim. Acta.* **2018**, *667*, 19–26. <https://doi.org/10.1016/j.tca.2018.04.010>.
- [4] P. Yin, J. H. Zhang, L. A. Mitchell, D. A. Parrish, J. M. Shreeve, 3,6-Dinitropyrazolo [4,3-c] pyrazole-based multipurpose energetic materials through versatile n-functionalization strategies, *Angew. Chem.* **2016**, *55*, 1–4. <https://doi.org/10.1002/anie.201606894>.
- [5] K. B. Landenberger, O. Bolton, A. J. Matzger, Two isostructural explosive cocrystals with significantly different thermodynamic stabilities, *Cryst. Eng.* **2013**, *125*, 6596–6599. <https://doi.org/10.1002/ange.201302814>.

- [6] Q. Huang, B. Jin, L. Q. Luo, Z. L. Guo, S. J. Chu, R. F. Peng, Isothermal decomposition kinetics and possible decomposition process of pentaerythritol tetranitrate, *J. Energ. Mater.* **2020**, 1–12. <https://doi.org/10.1080/07370652.2020.1787559>.
- [7] C. L. He, J. H. Zhang, D. A. Parrish, J. M. Shreeve, 4-Chloro-3,5-dinitropyrazole: a precursor for promising insensitive energetic compounds, *J. Mater. Chem. A* **2013**, 1, 2863–2868. <https://doi.org/10.1039/c2ta01359b>.
- [8] Q. Ma, H. C. Lu, L. Y. Liao, G. J. Fan, J. L. Huang, One-pot synthesis, crystal structure, and thermal decomposition behavior of 1,1'-diamino-4,4',5,5'-tetranitro-2,2'-biimidazole, *J. Energ. Mater.* **2017**, 35, 239–249. <https://doi.org/10.1080/07370652.2016.1267278>.
- [9] L. Z. Chen, W. Liu, J. L. Wang, D. L. Cao, Crystal structure and thermal decomposition kinetics of 3-nitro-4-diazo-5-oxygen-pyrazole, *Chinese J. Struct. Chem.* **2018**, 37, 1087–1092. <https://doi.org/10.14102/j.cnki.0254-5861.2011-1881>.
- [10] T. Golofit, M. Szala, Ł. Gutowski, M. Zybert, Studies on the thermal behaviour and safety of a novel thermostable explosive 5,5',6,6'-tetranitro-2,2'-bibenzimidazole, *Thermochim. Acta* **2018**, 668, 126–131. <https://doi.org/10.1016/j.tca.2018.08.019>.
- [11] Q. Huang, X. W. Liu, Y. Y. Xiao, L. Q. Luo, G. Luo, B. Jin, R. F. Peng, S. J. Chu, Isothermal thermal decomposition of the HMX based PBX explosive JOL-1, *J. Energ. Mater.* **2020**, 39, 1–9. <https://doi.org/10.1080/07370652.2020.1737988>.
- [12] J. Ai, J. J. Li, J. B. Chen, J. Chen, Q. Yu, Y. Xiong, Kinetics of thermal decomposition reaction of LLM-105 based PBX explosives, *Chinese Journal of Explosives & Propellants* **2016**, 39, 37–41. <https://doi.org/10.14077/j.issn.1007-7812.2016.04.007>.
- [13] C. E. S. Bernardes, A. Josephl, M. E. M. D. Piedade, Some practical aspects of heat capacity determination by differential scanning calorimetry, *Thermochim. Acta* **2020**, 687, 1–7. <https://doi.org/10.1016/j.tca.2020.178574>.
- [14] P. L. Wang, J. Q. Wang, J. L. Wang, Crystal structure and thermal decomposition kinetics of 1,3,5-trinitro-4,6-diazidobenzene, *J. Therm. Anal. Calorim.* **2021**, 143, 3983–3995. <https://doi.org/10.1007/s10973-020-09339-x>.
- [15] J. Bergman, T. Brimert, Synthesis and reactions of some dinitrodiazoquinones, *Tetrahedron* **1999**, 55, 5581–5592. [https://doi.org/10.1016/S0040-4020\(99\)00223-9](https://doi.org/10.1016/S0040-4020(99)00223-9).
- [16] T. M. Klapötke, K. Polborn, C. Rienäcker, Structure and bonding in 2-diazo-4,6-dinitrophenol (DDNP), *Propell. Explos. Pyrot.* **2003**, 28, 153–156. <https://doi.org/10.1002/prep.200390022>.
- [17] T. M. Klapötke, A. Preimesser, J. Stierstorfer, Synthesis and energetic properties of 4-diazo-2,6-dinitrophenol and 6-diazo-3-hydroxy-2,4-dinitrophenol, *Eur. J. Org. Chem.* **2015**, 20, 4311–4315. <https://doi.org/10.1002/ejoc.201500465>.
- [18] R. L. Atkins, W. S. Wilson, Synthesis of polynitrodiazophenols, *J. Org. Chem.* **1986**, 51, 2572–2578. <https://doi.org/10.1021/jo00363a032>.
- [19] X. M. Yang, X. Y. Lin, L. Yang, T. L. Zhang, A novel method to synthesize stable nitrogen-rich polynitrobenzenes with π -stacking for high-energy-density energetic materials, *Chem. Comm.* **2018**, 54, 10296–10299. <https://doi.org/10.1039/x0xx00000x>.
- [20] J. G. Wang, Y. Q. Zou, Synthesis and characterization of N-methyl-2,6-dinitrodiphenylamine-4-diazonium salt and its diazoresin, *J. Appl. Polym. Sci.* **2012**, 127, 4850–4857. <https://doi.org/10.1002/APP.38079>.
- [21] GJB 5891. National Military Standards of the People's Republic of China: Methods of test for explosive agents. Beijing: *Commission of Science and Technology for National Defense*. **2006**, 131–166.
- [22] GJB 772A-97. National Military Standards of the People's Republic of China: Methods of test for explosive agents. Beijing: *Commission of Science and Technology for National Defense*. **1997**, 184–247.
- [23] H. F. Wang, The crystal structure of 3,5-dichloro-6-diazo-2,4-dinitrocyclohexa-2,4-dien-1-one, *C₆Cl₂N₄O₅, Z Krist.-New Cryst. St.* **2021**, 236, 213–214. <https://doi.org/10.1515/ncrs-2020-0491>.
- [24] O. V. Dolomanov, L. J. Bourhis, R. J. Gildea, OLEX2: a complete structure solution, refinement and analysis program, *J. Appl. Cryst.* **2009**, 42, 339–341.
- [25] G. M. Sheldrick, SHELXT—Integrated space-group and crystal structure determination, *Acta. Cryst. A* **2015**, 71, 3–8.
- [26] G. M. Sheldrick, Crystal structure refinement with SHELXL, *Acta. Cryst. C* **2015**, 71, 3–8.
- [27] Y. L. Li, T. Y. Liu, D. L. Cao, J. L. Wang, Theoretical study on structure and properties of tetranitropyrrole and its derivatives, *Chinese J. Energ. Mater.* **2017**, 25, 291–297. <https://doi.org/10.11943/j.issn.1006-9941.2017.04.004>.
- [28] L. Li, B. S. Tan, R. F. Peng, B. Jin, S. J. Chu, Calculations of standard heat of formation and detonation parameters of 1,1,3,3-tetranitrocyclobutane, *Southwest University of Science and Technology*, **2010**, 25, 5–8. ISSN: 1671–8755.
- [29] J. Chen, P. B. Lian, L. Z. Chen, J. L. Wang, J. Chen, Crystal structure and thermal behaviour of imidazolium 2,4,5-trinitroimidazolate, *Cent. Eur. J. Energ. Mater.* **2019**, 16, 547–563. <https://doi.org/10.22211/cejem/113123>.
- [30] G. L. Zhao, Estimation of thermodynamic data of organic matter, Beijing: Higher Education Publishing Society, **1983**, 112–113.
- [31] H. E. Kissinger, Reaction kinetics in differential thermal analysis, *Anal. Chem.* **1957**, 29, 1702–1706. <https://doi.org/10.1021/ac60131a045>.
- [32] T. Ozawa, A new-method of analyzing thermogravimetric data, *Bull. Chem. Soc. Jpn.* **1965**, 38, 1881–1886. <https://doi.org/10.1246/bcsj.38.1881>.
- [33] J. Li, L. Z. Chen, J. L. Wang, G. C. Lan, H. Hou, M. Li, Crystal structure and thermal decomposition kinetics of byproduct of synthesis of RDX: 3,5-dinitro-1-oxygen-3,5-diazacyclohexane, *Acta. Phys-Chim. Sin.* **2015**, 31, 2049–2056. <https://doi.org/10.3866/PKU.WHXB201510092>.
- [34] L. Gigante, A. Lunghi, S. Martinelli, P. Cardillo, Calorimetric approach and simulation for scale-up of a friedel-crafts reaction, *Org. Process Res. Dev.* **2003**, 7, 1079–1082. <https://doi.org/10.1021/op030043a>.
- [35] J. Li, S. H. Jin, F. Bao, G. C. Lan, X. J. Wang, Q. H. Shu, B. P. Lu, K. Chen, Thermal safety assessment and thermo kinetic parameters of 5,5'-dinitramino 3,3'-bi[1,2,4-triazolate] carbonylhydrazide salt (CBNT), *J. Therm. Anal. Calorim.* **2021**, 114, 647–655. <https://doi.org/10.1007/s10973-020-09514-0>.

Manuscript received: January 5, 2021
 Revised manuscript received: May 8, 2021
 Version of record online: June 26, 2021